Philosophical Magazine
Vol. 89, Nos. 28–30, 1–21 October 2009, 2645–2654

Taylor & Francis
Taylor & Francis Group

Effect of bottom cell properties on micromorph tandem device performance

Paola Delli Veneri*, Lucia V. Mercaldo and Carlo Privato

ENEA-Portici Research Centre, P.leE. Fermi, 80055 Portici (Napoli), Italy

(Received 29 September 2008; final version received 29 January 2009)

Micromorph tandem solar cells represent an elegant way of overcoming the efficiency limits of single-junction solar cells and reducing the light-induced degradation of amorphous silicon films. Micromorph devices have been realised on Asahi U-type TCO-covered glass substrates by very high frequency plasma-enhanced chemical vapour deposition (VHF-PECVD) at 100 MHz at low substrate temperature (150°C). For the bottom cell, different growth regimes were explored by changing both chamber pressure and plasma power, with the aim of finding interesting regimes for industrial application. The effect of the structural composition of the microcrystalline absorber layer on the electrical parameters of the device was investigated. The highest efficiency (11.1%) is reached at 67 Pa and power to pressure ratio of 0.3 W/Pa. On the other hand, using a larger power to pressure ratio (0.5 W/Pa), high short circuit current density and constant efficiency over a wide silane concentration range were obtained. Homogeneity problems and low response at high wavelengths were found at large pressure (200 Pa). An evaluation of micromorph device stability was also carried out.

Keywords: thin film solar cell; microcrystalline hydrogenated silicon; tandem device

1. Introduction

Micromorph tandem solar cells, stacked structures consisting of a high band gap (1.7 eV) p-i-n amorphous silicon cell on top of a low band gap (1.1 eV) p-i-n microcrystalline silicon cell, were first introduced by IMT Neuchatel [1]. These devices combine the advantages of amorphous silicon and its technology with the stability and spectral sensitivity at long wavelengths of microcrystalline silicon. High efficiencies have indeed been reported by several research groups [1–3] and recent progress in up-scaling has led to production announcements [4–7]. However, since the properties of the microcrystalline material are strongly influenced by deposition conditions, a deeper understanding of the growth regimes is needed in order to make these devices competitive at industrial level. Moreover, the behaviour of micromorph devices under light soaking is an important issue that needs to be addressed. As a matter of fact, the best microcrystalline cells are deposited around the transition from crystalline to

*Corresponding author. Email: paola.dellivenеri@portici.enea.it

ISSN 1478–6435 print/ISSN 1478–6443 online

DOI: 10.1080/14786430902785344
http://www.informaworld.com

amorphous growth [8], and then both top and bottom cells might in principle contribute to the degradation effect in the overall device.

In this paper, an investigation is reported of micromorph tandem solar cells with different bottom cells grown by very high frequency plasma-enhanced chemical vapour deposition (VHF-PECVD). A low deposition temperature (150°C) was selected, in order to easily transfer this technology to low-cost plastic substrates in a future step. The single cell components were also analysed in view of their utilisation within the tandem structure. For the microcrystalline bottom cell, two different growth regimes, characterised by two values of plasma power to chamber pressure ratios, were explored. Materials with different structural composition were taken into account as intrinsic absorber layers, by using different silane concentrations in the gas mixture. An efficiency of 11.1% was achieved, and an interesting regime for industrial application has been evidenced. The devices have also been light-soaked for 200 h and a dependence of the efficiency loss on the crystallinity of the bottom absorber layer has been detected.

2. Experimental

Micromorph tandem solar cells were deposited on $10 \times 10\,cm^2$ Asahi U-type TCO-covered glass substrates. The top p-i-n structure consists of a 7 nm thick amorphous silicon carbide p-layer, a 270 nm thick amorphous silicon i-layer and a 30 nm thick microcrystalline n-layer. The bottom cell consists of a 30 nm thick microcrystalline p-layer, a 1.5 μm thick microcrystalline i-layer and a 40 nm thick microcrystalline n-layer. A ZnO back-reflector, followed by 1 cm × 1 cm Ag pads, was deposited.

The intrinsic layers of both the amorphous top cell and microcrystalline bottom cell were grown by VHF-PECVD at 100 MHz at low substrate temperature (150°C). The electrode configuration consists of a $13 \times 13\,cm^2$ powered electrode and an $11 \times 11\,cm^2$ substrate carrier as the grounded electrode. The inter-electrode distance was kept at 15 mm, and the gas supply was a simple cross-flow geometry. The plasma power and chamber pressure were kept, respectively, at 5 W and 27 Pa in the amorphous case, whereas different growth regimes were explored in the microcrystalline case. The pressure was varied from 40 to 200 Pa, and correspondingly the power was raised from 12 up to 60 W. In particular, two regimes characterised by power to pressure ratio equal to 0.3 W/Pa and 0.5 W/Pa were selected for investigation. The material was deposited with different silane concentrations ($SC = SiH_4/(SiH_4 + H_2) = 4.8 - 8.2\%$) in order to be in the so-called amorphous-to-microcrystalline transition regime [8]. The deposition rate, evaluated from thickness measurements performed by a step profiler, varied from $\sim 3\,Å\,s^{-1}$ at low pressure (40 and 67 Pa) to ~ 7–$8\,Å\,s^{-1}$ at 200 Pa.

Doped layers were grown by conventional RF-PECVD technique (13.56 MHz) in a separate chamber of the same cluster-tool deposition system, using phosphine and diborane as dopant gases to prepare n-type and p-type materials, respectively. Details about deposition parameters and properties of the doped layers are published elsewhere [9].

Some properties of the single-component cells were also investigated. H_2-diluted and undiluted amorphous silicon single junctions ($H_2/SiH_4 = 0, 2, 9$)

were first fabricated in order to study the effect of different band gaps on the current–voltage (J–V) characteristic. Transmission measurements, using a Perkin Elmer λ-900 spectrophotometer, were also performed on intrinsic amorphous silicon thin films in order to measure the parameter E_{04} (energy value corresponding to $\alpha = 10^4\,\mathrm{cm}^{-1}$). Microcrystalline p-i-n single junctions with different p-layers were fabricated: in particular two values of hydrogen dilution, $H_2/(H_2+SiH_4) = 99\%$ and 99.3%, were selected. The 1 μm thick absorber layer was deposited under the same conditions (67 Pa, 20 W and SC = 5.2%).

The devices were characterised by measuring spectral response and J–V characteristics under AM1.5 illumination. Variable intensity measurements (VIM), i.e. J–V curves at 0.01–100 mW cm^{-2}, were performed in order to evaluate the shunt resistance [10]. The light-soaking was carried out at open circuit under an AM 1.5 solar simulator for 200 h at 30°C. The crystallinity of the devices was also probed by determining the Raman spectra with the strongly absorbed 514 nm line of an Ar^+ laser and/or the weakly absorbed 633 nm line of a He–Ne laser. The crystalline and amorphous phase fractions were evaluated using $\Phi_c = (I_{520}+I_{510})/(I_{520}+I_{510}+I_{480})$ and $\Phi_a = I_{480}/(I_{520}+I_{510}+I_{480})$, respectively, where I_i is the area under the peak centred at wavenumber, i [11].

3. Results and discussion

3.1. *Single-component cells*

When fabricating a micromorph tandem solar cell, the basic problem is combining a high-current but low-voltage microcrystalline cell with a low-current but high-voltage amorphous cell. We first focused on the amorphous top cell. It is known that amorphous silicon deposited with hydrogen dilution has enhanced stability against light soaking [12]. However, hydrogen dilution reduces the optical absorption, and this causes lower current densities [13].

We included different types of amorphous material as absorber layer in single p-i-n junctions, in order to evaluate the effect of different band gaps on the J–V characteristic. In Table 1 we report the E_{04} values determined by transmission experiments on films deposited with different hydrogen to silane flow ratios in the gas mixture. The higher optical gap of the H_2-diluted material translates into larger open circuit voltage, but lower short circuit current (J_{SC}), as shown in the same table. In order to enhance the efficiency of micromorph tandem cells the optical absorption in the top cell must be increased. As a matter of fact, due to the high current potential of the microcrystalline bottom cell, it is preferable to optimise the top cell in order to obtain a high current rather than a high voltage. Therefore, as already done elsewhere [13], undiluted amorphous silicon was chosen to be inserted in the top cell of the tandem devices. In our case, however, the absorber material was grown at lower substrate temperature (150°C), which still allows for a sufficiently high short circuit current density.

Moreover, for both the single-component cells special attention must be paid on the p-layer. Since optical absorption within the p-layer can limit J_{SC}, material with wide optical gap is desired. At the same time, this layer has to be highly

Table 1. Hydrogen to silane flow ratio and optical gap (E_{04}) for one undiluted and two H_2-diluted amorphous silicon samples, together with the open circuit voltage and short circuit current density of three amorphous p-i-n solar cells characterised by the three different absorber layers.

Amorphous i-layers		Solar cells	
H_2/SiH_4	E_{04} (eV)	V_{OC} (mV)	J_{SC} (mA cm^{-2})
0	1.92	860	13.8
2	1.95	870	13.1
9	1.98	885	11.1

Table 2. Structural and electrical parameters of p-i-n microcrystalline solar cells with p-doped layers grown with two different hydrogen dilutions.

	$H_2/(H_2+SiH_4)$ (%)	Φ_C (%)	FF (%)	V_{OC} (mV)	J_{SC} (mA cm^{-2})	R_{Sh} (kΩ cm^2)
M-P1	99.0	60	62.0	486	20.1	6
M-P2	99.3	68	61.7	475	19.2	3

conducting and, for microcrystalline p-i-n solar cells, sufficiently crystalline to promote the nucleation of the superimposed microcrystalline i layer at the p/i interface [14].

However, too large crystalline phase fraction could also be deleterious, as illustrated in Table 2. Here structural and electrical parameters of two microcrystalline p-i-n solar cells with different p-layers, grown with two different values of hydrogen dilution, are reported. The crystalline phase fraction, Φ_c, in Table 2 was evaluated through Raman analysis, with focused Ar^+ laser (514 nm) arriving through the glass substrate and the TCO (transparent conducting oxide) on the first-deposited silicon p-layer of the device. The collected Raman contribution arises from the doped layer (about 25 nm) and the first tens of nanometres of the i-layer [11]. The overall device performance is worse for the cell that includes a more crystalline p-layer (M-P2), and the quantum efficiency (Figure 1) shows a clear loss in the low wavelength range (360–600 nm) for this device.

By using the variable illumination measurement (VIM) technique [10] at very low illumination levels, a lower shunt resistance (R_{Sh}) was evaluated for device M-P2 (3 kΩ cm^2) (Table 2). Then, a possible correlation between large crystalline phase fraction in the p-layer and formation of cracks can be advanced. The presence of cracks through the p-layer and the first part of the absorber layer close to the p/i interface could explain the reduced spectral response and the lower V_{OC}. Moreover, the presence of cracks could favour boron diffusion and give rise to a thicker effective p-layer, which would contribute to the reduced quantum efficiency in the blue-green wavelength range.

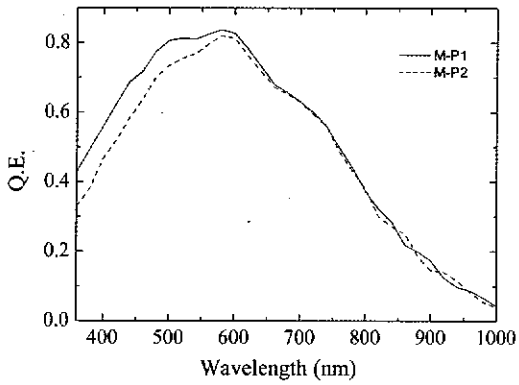

Figure 1. Spectral response of the microcrystalline p-i-n solar cells with the p-doped layers described in Table 2.

Summarising, undiluted amorphous silicon deposited at low temperature (150°C) is selected as absorber layer for the top cell. The window p-layers need special care: in particular for the microcrystalline component cell a crystalline phase fraction for such doped layer around 60% has been chosen to avoid possible formation of cracks at the interface with the i-layer.

3.2. *Tandem devices*

For each pressure value a series of tandem cells was fabricated with the intrinsic layer in the bottom cell grown with different silane concentration values, in order to study the effect of the structural composition on the device performance and find the optimum phase mixture. Such material, which results in the highest solar cell efficiency, is found within the transition region from crystalline to amorphous growth [8]. The thickness of the active layers was fixed to 270 nm for the top cell and 1.5 μm for the bottom cell. In all cases the fabrication conditions for the top cell were never changed; therefore all the variations observed in the photovoltaic parameters are due to the bottom cell. Table 3 shows the main deposition parameters of the bottom absorber layer of the five series discussed, realised by using a power to pressure ratio equal to 0.3 W/Pa (series name ending with A) or 0.5 W/Pa (series name ending with B).

The electrical parameters extracted from the J–V characteristics of the cells are shown in Figure 2. The amorphous to crystalline transition region is determined by all the deposition parameters, therefore the relative positions of all the curves along the SC axis are not always significant. In all cases FF, J_{SC} and the efficiency first increase with silane concentration and then drop after reaching their maximum values, whereas V_{OC} monotonously increases with SC and is approximately equal to the sum of the V_{OC} values of the single cells (Tables 1 and 2), thus evidencing negligible losses at the tunnel recombination junction.

Looking at the A-type series first (solid symbols in Figure 2), pronounced peaks for J_{SC}, FF and η are observed. The maximum J_{SC} values are almost the same in all

Table 3. Chamber pressure, plasma power and silane concentration (SC) range used to deposit the series of tandem devices.

Series	Pressure (Pa)	Power (W)	Power/pressure (W/Pa)	SC (%)
T40A	40	12	0.3	5.5–7.0
T67A	67	20	0.3	5.5–7.2
T200A	200	60	0.3	5.5–6.7
T40B	40	20	0.5	4.8–8.0
T67B	67	33	0.5	5.2–8.2

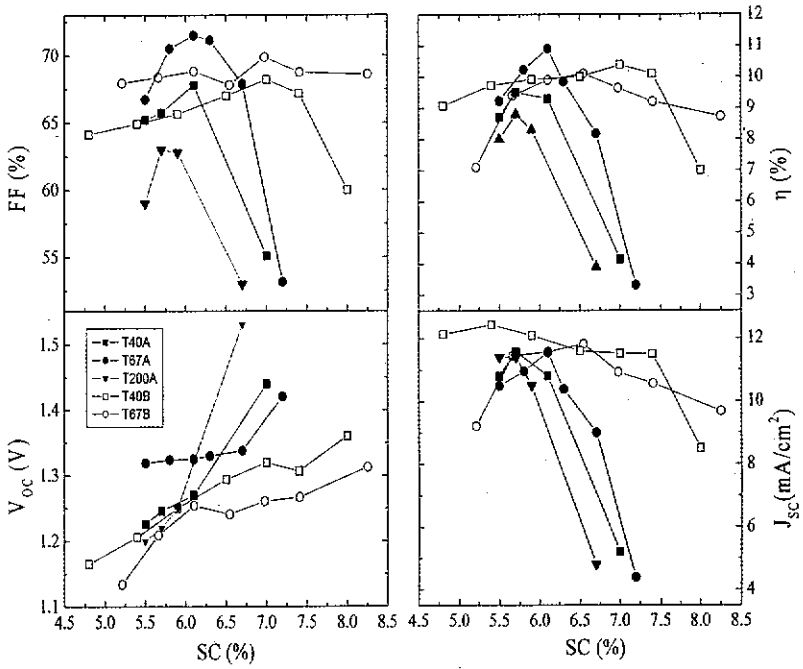

Figure 2. Electrical parameters extracted from the *J–V* characteristics under AM1.5 illumination of the five silane concentration series of tandem cells described in Table 3. Solid and open symbols refer to series grown at power to pressure values of 0.3 W/Pa and 0.5 W/Pa, respectively. The lines are guides for the eye.

cases (11.6–11.8 mA cm^{-2}). However, an overall improvement is registered when the pressure is raised from 40 to 67 Pa, whereas at much larger pressure (200 Pa, series T200A) a general deterioration of all the parameters is found. The worse electrical parameters found for series T40A could be related to the low power (12 W), maybe not sufficient to grow a good quality microcrystalline material with low defect density. Poor quality of the bottom absorber material can be expected also in the high pressure regime, due to the larger growth rate. As a matter of fact, quantum efficiency measurements on the bottom cell of devices from series T200A show a low

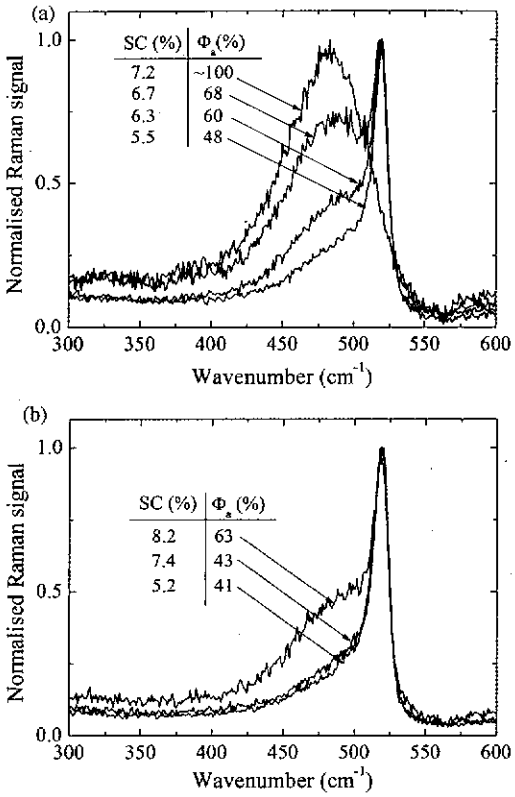

Figure 3. Normalised Raman spectra of tandem solar cells from series T67A (a) and T67B (b) obtained with the weakly absorbed 633 nm excitation light arriving on the last deposited n-layer. The amorphous phase fraction, Φ_a, is also reported in the figures.

response for the red and near-infrared wavelengths, as already reported in the literature [15]. Moreover, at 200 Pa some difference in the performance among the devices realised on the $10 \times 10\,cm^2$ substrate, excluding the cells positioned in the central part of the substrate, is present due to structural and thickness inhomogeneity. For all these reasons no B-type series was realised at high pressure.

Both the B-type series (open symbols in Figure 2) have large current values and almost constant FF and η in a wide SC range. However, lower V_{OC} values have been obtained with respect to the A-type series, due to the worse p/i interface when high power to pressure ratio is used to grow the bottom absorber material. The lowest V_{OC} values have been found for series T67B, thus giving indication of further worsening of the p/i interface when high power is used.

The main difference among A- and B-type series resides in the wideness of the amorphous to crystalline phase transition region, as confirmed by Raman analysis. In Figure 3 the spectra obtained with focused excitation light (633 nm) arriving on the last-deposited silicon n-layer are shown for the two series deposited at 67 Pa and different power levels. In this case the collected Raman contribution arises from the doped layer (about 40 nm) and about half of the microcrystalline i-layer [11],

and then it gives a good indication of the crystallinity of the bottom absorber layer. For series T67B (Figure 3b) the crystalline phase fraction is practically the same in a wide SC range (5.2–7.4%), whereas in the same range a rapid variation of crystalline phase fraction is observed for series T67A (Figure 3a). In this last case Raman analysis reveals a mixed material ($\Phi_a = 48\%$) at SC = 5.5% and an almost totally amorphous material at SC = 7.2%. Moreover, generally larger crystalline phase fractions are registered in the B-type series.

A peculiar behaviour of series T40B ought to be pointed out, namely the large short circuit current density (up to 12.4 mA cm^{-2} at SC = 5.4%) even if Raman analysis reveals a narrower transition region when compared to series T67B. In particular, the large current densities measured in this case are obtained with bottom absorber materials characterised by crystallinity values between 36% and 64%. This means that even with relatively low crystalline phase fractions it is possible to generate/collect large currents. Since this series has the same doped layers and back reflector as the others, we do not expect enhanced light scattering at the back reflector or improved efficiency of carrier collection. Therefore, these larger currents can be explained by means of a bulk material with a structure particularly apt to scatter the impinging radiation within the device and then optimise the absorption and carrier generation [16]. This assumption finds a confirmation in the spectral response of the cells of series T40B. Figure 4 shows the quantum yield of the best cell of series T40B (SC = 5.9%) and T67A (SC = 6.1%). As expected no change is observed for the top cell, whereas the bottom cell from series T40B shows a larger response for the red and near-infrared wavelengths, which can be interpreted in terms of a better absorption of the radiation within the bottom microcrystalline i-layer.

The large currents measured on series T40B are not accompanied by sufficiently high V_{OC} values. In the micromorph structure, due to the low current of the top cell, it is preferable, within some limits, to choose an absorber material for the bottom cell that furnishes a high voltage rather than a high current. Therefore, the efficiency is maximised within series T67A (11.1%), where generally larger V_{OC} values are

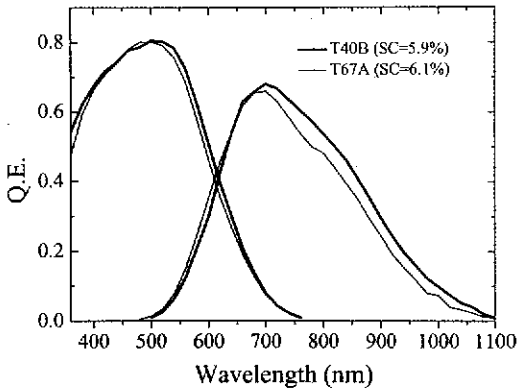

Figure 4. Spectral response of the best micromorph tandem devices from series T40B and T67A.

obtained, coupled with FF > 70%. However, we want to point out that such a growth regime is characterised by a more pronounced dependence on SC. The weak dependence of J_{SC}, FF and η on silane concentration found when using high power to pressure ratio (0.5 W/Pa), makes this condition very interesting for industrial application, where a precise control of gas concentration on large areas can be difficult.

Finally, the stability of the micromorph devices has been evaluated by exposing the cells to white light for 200 h, a sufficiently long time to extract meaningful indications on the light-soaked state, even if saturation is not yet reached. As expected, lower relative efficiency loss, $\Delta\eta = (\eta_{initial} - \eta_{degraded})/\eta_{initial}$, is found when Φ_c in the bottom cell is larger, due to the stability of the crystalline phase. Generally, $\Delta\eta$ ranges in between 5 and 9%, depending on Φ_c. Larger efficiency losses ($\Delta\eta \sim 13\%$) have been registered only for the devices from series T40B grown at low SC that appear top cell (more unstable) limited devices from QE measurements. In fact, the opposite condition, with the more stable component cell limiting the output current, was already shown to significantly improve the stability of tandem devices [17]. We can conclude that, due to the better stability of the microcrystalline component cell, a bottom cell limited current mismatch is preferable in micromorph devices in order to contain the light-induced degradation effect. In this condition the best devices have $\Delta\eta < 6\%$.

4. Conclusions

Micromorph tandem solar cells have been fabricated by VHF-PECVD at 100 MHz at low deposition temperature (150°C). Undiluted amorphous silicon was chosen as the optimal absorber layer for the top cell, because of its lower band gap, allowing for larger currents. An optimal crystallinity for the p-layer within the microcrystalline component cell has been evaluated around 60%, to avoid possible formation of cracks at the interface with the i-layer, evidenced with larger crystalline phase fraction. Different deposition regimes for the bottom cell within the micromorph device have been investigated. The power to pressure ratio has been identified as an important parameter. The best performance, with an initial efficiency of 11.1%, has been found at low power to pressure ratio (0.3 W/Pa), when growing the bottom absorber layer at 67 Pa, due to the larger V_{OC} and FF values obtained in this regime. At much larger pressure (200 Pa), where interestingly high deposition rates ($\sim$7–8 Å s^{-1}) are obtained, absorber material with low response at red and near-infrared wavelengths is grown and some homogeneity problems are evidenced on the $10 \times 10\,cm^2$ substrate area. In the large power to pressure ratio regime (0.5 W/Pa), devices with high short circuit current density and constant FF in a wide SC range are obtained. In particular, a J_{SC} of 12.4 mA cm^{-2} has been reached at 40 Pa. The weak dependence of J_{SC}, FFη and on silane concentration makes this regime very interesting for industrial application, where the production of large area devices asks for non-trivial control of gas-distribution uniformity. Finally, light-soaking of the tandem solar cells has shown that the efficiency loss depends on the crystallinity of the bottom absorber layer, and devices with a bottom cell limited current mismatch are preferable in order to maintain high efficiency in the degraded state. In this

condition, after 200 h an efficiency loss lower than 6% has been measured on the best solar cells.

References

[1] J. Meier, S. Dubail, R. Flückiger, D. Fischer, H. Keppner and A. Shah, *Proceedings of the First World Conference on Photovoltaic Energy Conversion*, Hawaii, USA, 1994, p.409.

[2] J. Meier, S. Dubail, S. Golay, U. Kroll, S. Faÿ, E. Vallat-Sauvain, L. Feitknecht, J. Dubail and A. Shah, Sol. Energ. Mater. Sol. Cell. 74 (2002) p.457.

[3] K. Yamamoto, M. Yoshimi, Y. Tawada, S. Fukuda, T. Sawada, T. Meguro, H. Takata, T. Suezaki, Y. Koi, K. Hayashi, T. Suzuki, M. Ichikawa and A. Nakajima, Sol. Energ. Mater. Sol. Cell. 74 (2002) p.449.

[4] M. Yoshimi, T. Sasaki, T. Sawada, T. Suezaki, T. Meguro, T. Matsuda, K. Santo, K. Wadano, M. Ichikawa, A. Nakajima and K. Yamamoto, *Conference Record of the 3rd World Conference on Photovoltaic Energy Conversion*, Osaka, May 2003, p.1566.

[5] U. Kroll, J. Meier and S. Benagli, *Proceedings of the 22nd European Photovoltaic Solar Energy Conference*, Milan, Italy, 3–7 September 2007, p.1795.

[6] Y. Chae, T.K. Won, L. Li, S. Sheng, S.Y. Choi and J. White, *Proceedings of the 22nd European Photovoltaic Solar Energy Conference*, Milan, Italy, 3–7 September 2007, p.1807.

[7] H. Takatsuka, *Proceedings of the 21st European Photovoltaic Solar Energy Conference*, Dresden, Germany, 4–8 September 2006, p.1531.

[8] O. Vetterl, F. Finger, R. Carius, P. Hapke, L. Houben, O. Kluth, A. Lambertz, A. Mück, B. Rech and H. Wagner, Sol. Energ. Mater. Sol. Cell. 62 (2000) p.97.

[9] P. Delli Veneri, L.V. Mercaldo, C. Minarini and C. Privato, Thin Solid Films 451–452 (2004) p.269.

[10] J. Merten, J.M. Asensi, C. Voz, A.V. Shah, R. Platz and J. Andreu, *IEEE Trans. Electron Dev.* 45 (1998) p.423.

[11] P. Delli Veneri, L.V. Mercaldo, P. Tassini and C. Privato, Thin Solid Films 487 (2005) p.174.

[12] S. Guha, K.L. Narasimhan and S.M. Pietruszko, J. Appl. Phys. 52 (1981) p.859.

[13] R. Platz, C. Hof, D. Fischer, J. Meier and A. Shah, Sol. Energ. Mater Sol. Cell. 53 (1998) p.1.

[14] S. Hamma and P. Roca i Cabarrocas, Sol. Energ. Mater. Sol. Cell. 69 (2001) p.217.

[15] U.S. Graf, J. Meier and A. Shah, *Proceedings of the Third World Conference on Photovoltaic Energy Conversion*, 2004, p.1663.

[16] A. Poruba, A. Fejfar, Z. Remeš, J. Špringer, M. Vaněček, J. Kočka, J. Meier, P. Torres and A. Shah, J. Appl. Phys. 88 (2000) p.148.

[17] B. Yan, G. Yue, J. Yang, K. Lord and S. Guha, Mater. Res. Soc. Symp. Proc. 762 (2003) p.309.